



REVIEW

Probe pulse design in Brillouin optical time-domain reflectometry

Mupeng Li¹ | Tianhua Xu^{1,2,3}  | Shuang Wang¹ | Wenxiu Hu²  |
Junfeng Jiang¹ | Tiegen Liu¹

¹School of Precision Instrument and Opto-Electronics Engineering, Tianjin University, Tianjin, China

²School of Engineering, University of Warwick, Coventry, UK

³Department of Electronic and Electrical Engineering, University College London, London, UK

Correspondence

Tianhua Xu and Junfeng Jiang School of Precision Instrument and Opto-Electronics Engineering, Tianjin University, Tianjin 300072, China.
Email: tianhua.xu@ieec.org and jiangjfxu@tju.edu.cn

Funding information

H2020 Marie Skłodowska-Curie Actions, Grant/Award Number: 101008280; National Natural Science Foundation of China, Grant/Award Number: 61735011

Abstract

Brillouin optical time-domain reflectometry (BOTDR) is a branch of distributed fibre-optic sensors, and it can measure the strain and the temperature information, localised by the return time of the probe pulse, along the fibre based on the spontaneous Brillouin scattering process. Parameters of the BOTDR system, including the spatial resolution, the signal-to-noise ratio, the measurement speed, and the sensing range, have a mutually restrictive relationship. In order to improve the performance of the BOTDR system, researchers have focussed on improving the design of the probe pulse, for example, transforming the shape, the sequence, and the spectral properties of the pulse. This study summarises the recent progress in the design of detection pulses in BOTDR systems, and comprehensively demonstrates the improvement effects of various pulse modulation formats on the system performance.

1 | Introduction

Over the past decades, optical fibre sensors have penetrated every aspect of human life, such as structural health monitoring [1], biosensing [2–4], acoustic monitoring [5–7], temperature sensing [8], et al. Optical fibre sensors can be divided into discrete sensing and distributed sensing [9]. The former schemes measure physical parameters at specified positions in optical fibres, such as the well-known fibre Fabry-Perot (FP) sensing [10], fibre surface plasmon sensing [11], grating sensing [12], and so on. The latter sensors illustrate a more attractive effect for spatial monitoring, which evaluate the information along the whole cable length, based on the optical interference as a fibre-optic Mach-Zehnder interferometer to measure the difference in the temperature (or the pressure) between two fibre arms [13], and optical scatterings including Rayleigh scattering, Brillouin scattering, and Raman scattering [14, 15]. Distributed optical fibre sensors (DOFSs) based on Rayleigh scattering currently become a hot research direction because

Rayleigh scattering is a linear scattering process and can lead to the highest scattering energy compared to other approaches. The first implementation of the optical time-domain reflectometry (OTDR) based on Rayleigh backscattered light has effectively detected the loss characteristics along the optical fibre to non-destructively extract the information, such as breakpoints, bends, and damages [16]. Meanwhile, the polarisation properties and the phase properties of Rayleigh scattered lightwave have also been explored on the basis of the OTDR structure [17]. DOFSs based on Raman scattering are commonly used to detect the temperature distribution along the optical fibre [18]. Although research works of DOFSs based on Brillouin scattering started relatively late, the technology has been rapidly developed due to the characteristics of Brillouin scattering that can simultaneously sense the temperature and the strain.

DOFSs based on Brillouin scattering are mainly focussed on the following four aspects: (I) The Brillouin frequency-domain analysis measures the impulse response function and

This is an open access article under the terms of the Creative Commons Attribution License, which permits use, distribution and reproduction in any medium, provided the original work is properly cited.

© 2022 The Authors. *IET Optoelectronics* published by John Wiley & Sons Ltd on behalf of The Institution of Engineering and Technology.

the complex transfer function of the optical fibre to determine the information of the along the optical fibre, which is time-consuming and computationally complex [19]. (II) The Brillouin optical correlation domain analysis can obtain millimetre-level spatial resolution by analysing the correlation function of the continuous pump wave and the probe pulse, but the sensing range is usually short [20]. The time-domain-based Brillouin DOFSs can better balance the above shortcomings. (III) The Brillouin optical time-domain analysis (BOTDA) adopts the structure of double-ended incidence based on stimulated Brillouin scattering (SBS) in the optical fibre while it still has the disadvantage of inconvenient maintenance in practical engineering applications [21]. (IV) The Brillouin optical time-domain reflectometry (BOTDR) system only employs a single-end structure to detect the spontaneous Brillouin scattering in the optical fibre. However, the intensity of the spontaneous Brillouin scattering is much lower than that of the SBS, and the frequency shift of Brillouin scattering is much smaller than that of Raman scattering. These increase the difficulty in the detection of Brillouin scattering. Important indicators to measure the performance of BOTDR system include the signal-to-noise ratio (SNR), the spatial resolution, the frequency accuracy and the sensing range etc. The properties, such as the intensity, the pulse width, and the spectral width of the probe pulse in the system will pose great impacts on these indicators. There will be trade-off between some indicators for a BOTDR system. For example, a narrower pulse can lead to a higher spatial resolution of the system, but if the pulse is over narrow, the Brillouin spectrum will be broadened, resulting in a lower frequency accuracy. Meanwhile, the increase of the probe pulse power can generally improve the SNR of the system. However, when the power of the incident light exceeds the SBS threshold, the induced SBS effect can degrade the performance of the system. The sensing range also depends closely on the SNR of the system.

To further improve and optimise the performance of the BOTDR system in various practical application scenarios, researchers have studied the injection of the probe pulse in the system. To improve the spatial resolution of the system, it is necessary to adjust and optimise the width of the probe pulse. In 2008, Koyamada et al. demonstrated that the dual-pulse wave can effectively improve the spatial resolution of the BOTDR. Different shapes of the detection pulses and the corresponding sensing systems have been comprehensively investigated. To overcome the restriction of the SBS threshold on the incident optical power of the system, the pulse coding technique has been applied into the BOTDR system since 2008. Although Golay coding and simplex coding sequences have been widely used in various DOFS systems, a novel scheme called Random coding was developed in 2022 with a higher coding gain achieved [22]. Many researchers have also proposed new designs on the study of the frequency of pulsed lasers. Traditional BOTDR systems mostly use narrow-bandwidth lasers to detect the Brillouin spectrum with a spectral width in the order of MHz. In Ref. [23], a distributed feedback laser is used to generate the pulse with a linewidth reduced to approximately 6 kHz. Since 2009, the BOTDR

system has adopted the wavelength multiplexing technique to extract and average multiple Brillouin spectra during one pulse emission process, in order to improve the SNR and measurement speed of the system. Furthermore, in recent years, the utilisation of the linear frequency modulation (LFM) technique in DOFSs has led to the multi-aspect improvement in the system performance [24, 25]. In 2021, a bipolar-chirped pulse was deployed in the BOTDR system. The application of the chirped pulse can improve the spatial resolution of the BOTDR system under certain conditions, but the frequency crosstalk constrained the accurate extraction of the information. In addition, some works have utilised other properties of pulses and have enhanced the performance of BOTDR systems. It has been shown that the performance of the probe pulse posed a great influence on the performance of the system.

In this paper, recent research works on the pulse design and improvement in the BOTDR technology will be reviewed systematically. Firstly, the basic principle of the BOTDR system is introduced, including the spontaneous Brillouin scattering in optical fibre, the structure of the BOTDR system, and the trade-off relationship between the parameters in the BOTDR system. Subsequent sections describe the designing schemes for single pulses or pulse pairs, applications of pulse coding, and frequency modulation schemes for optical pulses. The pulse design scheme of BOTDR is summarised and prospected.

2 | THEORETICAL BACKGROUND

2.1 | Brillouin scattering in optical fibre

In general, the light scattering in optical fibres can be divided into three categories: Rayleigh scattering, Brillouin scattering, and Raman scattering. Rayleigh scattering is the most efficient scattering and is known as quasi-elastic scattering, which is generated by non-propagating density fluctuations in the optical fibre with no frequency shift. Brillouin and Raman scattering are called inelastic scattering, generated by the non-linear optical response of the energy and the momentum exchanges between the incident light and the fibre material. These exchanges arise from the material vibrations excited by the thermal excitation, and the phonons scale in each possible vibrational wave with the quantity difference according to their frequency and the ambient temperature. The incident optical wave thus finds a material wave in matching the resonance and imposes a frequency shift through the Doppler effect such a phenomenon is called the spontaneous scattering [26]. When material fluctuations are induced by the extra optical fields, such light scattering is named as the stimulated process (with higher efficiency) rather than the spontaneous light scattering. Phonons can be divided into two branches: Raman scattering is considered as the optical branch and the Brillouin scattering is classified into the acoustic branch, according to the different energy and interactions of phonons in the optical fibre. The optical power of inelastically scattered light depends on the

number of phonons. The peak power of Raman scattered light is extremely weak due to the small number of optical phonons. The power and the frequency shifts of the three scattered optical waves are shown in Figure 1. Those components shifted to lower frequencies are defined as Stokes components, and those components shifted to higher frequencies are named as anti-Stokes components.

A strict phase-matching condition should be satisfied to realise spontaneous Brillouin scattering in the optical fibre, based on the momentum conservation among the incident lightwave, scattered lightwave, and the acoustic wave. The Brillouin frequency shift (BFS) ν_B is highly dependent on the scattering angle θ . The approximate calculation formula is as follows.

$$\nu_B \approx \frac{2V_a n_{\text{eff}}}{\lambda_p} \sin \frac{\theta}{2} \quad (1)$$

where n_{eff} is the effective refractive index of the optical fibre, λ_p is the wavelength of the probe pulse, and V_a is the velocity of the longitudinal acoustic waves in the fibre, which can be determined as

$$V_a = \sqrt{\frac{Y(1-\kappa)}{(1+\kappa)(1-2\kappa)\rho}} \quad (2)$$

where Y is the Young's modulus, ρ is the fibre density, κ is the Poisson's ratio, which is sensitive to both the temperature and the strain in optical fibre. In a single-mode optical fibre, there are only two propagation directions of the scattered wave to the incident wave: parallel ($\theta = 0$) or anti-parallel ($\theta = \pi$). Considering the scheme of the forward scattered lightwave ($\theta = 0$), the frequency shift is zero. That means Brillouin scattering poses no effect in the forward direction. For the backward scattered lightwave ($\theta = \pi$), the value of BFS ν_B can be calculated as

$$\nu_B = \frac{2V_a n_{\text{eff}}}{\lambda_p} \quad (3)$$

In a single-mode fibre, Brillouin scattering exhibits the maximum frequency shift ν_B of approximately 11-GHz at

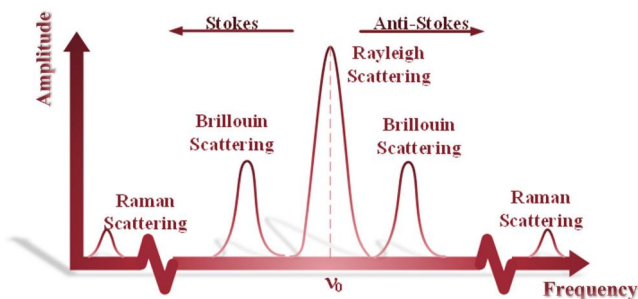


FIGURE 1 Schematic of the frequencies and intensities in the three types of scattering in optical fibres.

$\lambda_p = 1550$ nm. The intensity of the spontaneous Brillouin scattered lightwave is two orders of magnitude lower than the Rayleigh scattering. The Brillouin backscattered-light power $P_B(z, \nu)$ is given in Ref. [27] as

$$P_B(z, \nu) = g(\nu, \nu_B) \left(\frac{c}{2n} \right) P \exp(-2\alpha_z z) \quad (4)$$

where c is the light velocity in vacuum, n is the refractive index of the optical fibre, P is the product of the width and the power of the launched optical pulse, α_z is the attenuation coefficient of the fibre, and $g(\nu, \nu_B)$ is the Brillouin gain which is given by

$$g(\nu, \nu_B) = \frac{g_0(\omega/2)^2}{(\nu - \nu_B)^2 + (\omega/2)^2} \quad (5)$$

where g_0 is the peak value of the Brillouin gain, ω is the full width at half maximum (FWHM) of the Brillouin spectrum, depending on the phonon lifetime τ_A as $\omega = 1/2\pi\tau_A$. Typically the phonon lifetime is 5.9 ns, and thus the FWHM of the Brillouin spectrum is 27 MHz.

The strain and the temperature in the fibre have an effect on the speed of sound, resulting in a change in the Brillouin shift. It has been proven that the variation of BFS ν_B has a linear relationship with the variation of the temperature T and the strain ϵ , which can be described in Ref. [28] as

$$\Delta\nu_B = C_T \Delta T + C_\epsilon \Delta\epsilon \quad (6)$$

where C_T and C_ϵ are the linear coefficients. According to experimental strain and temperature measurements, the values of the two coefficients at the wavelength of 1.55 μm are typically $C_T = 1.18$ MHz/ $^\circ\text{C}$ and $C_\epsilon = 0.048$ MHz/ $\mu\epsilon$ respectively [29].

2.2 | Brillouin optical time-domain reflectometry

OTDR is a traditional scheme of DOFSs, based on Rayleigh scattering in the optical fibre [16, 30]. A typical OTDR setup is illustrated in Figure 2. A probe pulse is launched into the optical fibre via a coupler at the initial time $t = 0$. As this pulse propagates in the test fibre, Rayleigh scattering occurs continuously at each position z to all directions components with the attenuation of the light power. A portion of this scattered light will travel backward and pass through the

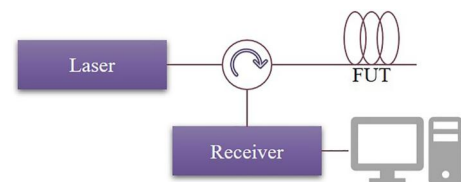


FIGURE 2 A typical OTDR setup. FUT, fibre under test; OTDR, optical time-domain reflectometry.

coupler before reaching the receiver, where the travelling time t_R of the pulse can be detected. Therefore, the distance between the scattered position and the starting point of the fibre can be converted by the travelling time t_R :

$$z = \frac{\nu_g t_R}{2} \quad (7)$$

where ν_g is the group velocity of the incident light in the optical fibre, the factor $\frac{1}{2}$ represents the round-trip propagation of the pulse. OTDR system is mainly used to detect the loss distribution along the optical fibre. When the physical properties of each point along the test non-destructive fibre are the same, the curve of Rayleigh scattered light power versus transmission distance decreases smoothly due to the inevitable fibre loss. By contrast, splice loss, connector insertion loss, and micro-bending loss will manifest as breakpoints on the curve to locate the points of fibre damage [31, 32].

Due to the low energy of the spontaneous Brillouin scattering in the fibre and the small value of BFS, the BOTDR system mostly adopts the coherent detection to improve the SNR of the system. There are currently three frequency sweeping methods to extract the Brillouin spectrum of the system: acousto-optical, electro-optical, and microwave heterodyne frequency shifting, as shown in Figure 3a–c respectively. The BOTDR system using the acousto-optic frequency shifting scheme is the first proposed BOTDR system [23, 33]. An acousto-optical modulator (AOM) was utilised to transform the continuous wave into a probe pulse. The AOM2 with an erbium-doped fibre amplifier (EDFA) constituted a frequency translation ring circuit to provide the frequency shift ν_S of about 11 GHz. A balanced photo-detection was used to receive the local reference light and the Brillouin backscattered light for the coherent detection to obtain the frequency difference $\nu_S - \nu_B$ between the two beams. The Brillouin scattering lightwave and the local reference light are performed as

$$E_B(\nu) = E_B \exp[i2\pi(\nu + \nu_S - \nu_B)t + \varphi_B] \quad (8)$$

$$E_L(\nu) = E_L \exp(i2\pi\nu t + \varphi_L) \quad (9)$$

Therefore, the photo-current in the balanced photodetector is proportional to

$$I \propto 2E_B E_L \cos[2\pi(\nu_S - \nu_B)t + (\varphi_B - \varphi_L)] \quad (10)$$

A electrical band pass filter with a fix central frequency is placed after the receiver, and the spectrum analysis process is accomplished by converting the frequency shift times of the probe pulse in the fibre loop.

In order to reduce the frequency error caused by the AOM and improve the stability of the system, electro-optical modulators (EOM) are currently used in the BOTDR system to realise pulse modulation in the detection optical path and frequency shifting of the reference optical path, so that the frequency difference in the receiver is limited to several MHz.

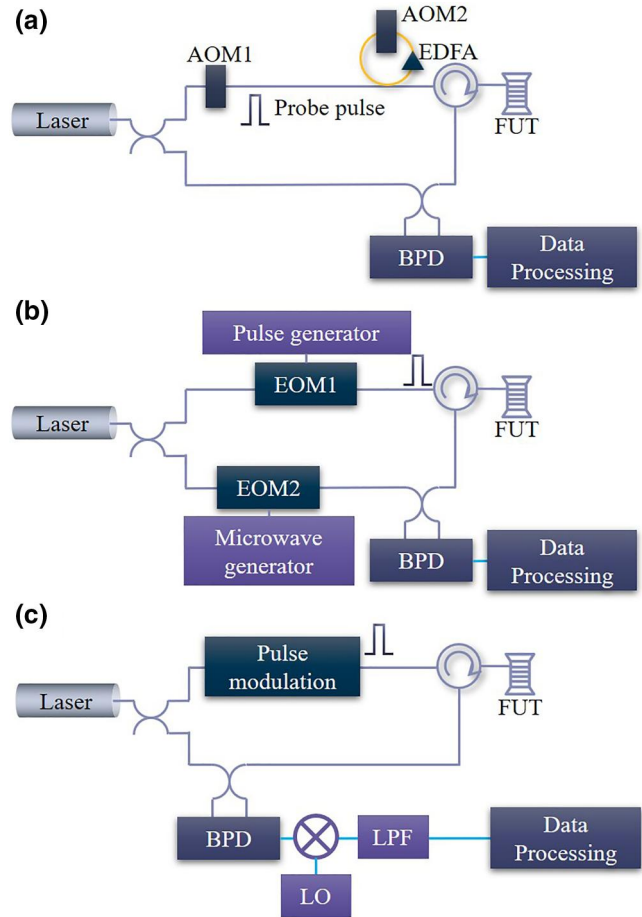


FIGURE 3 The setup of BOTDR systems with different frequency detection scheme. (a) Acousto-optical frequency shifting scheme. (b) electro-optical frequency shifting scheme. (c) Microwave heterodyne frequency shifting scheme. BOTDR, Brillouin optical time-domain reflectometry; BPD, balanced photodetector; LO, local oscillator; LPF, low pass filter.

In addition, the combination of the EOM and the arbitrary waveform generators can modulate the probe pulse with different shapes, phases, and frequency ranges, which also puts a considerable impact on the improvement of the BOTDR system performance.

The microwave heterodyne frequency shifting method is to directly obtain the frequency difference between the pulse optical path and the reference optical path, that is, the BFS ν_B in the fibre, and to mix the high frequency signal obtained by the receiver with the local oscillator (LO) signal in the circuit module. The frequency sweeping is achieved by continuously changing the frequency of the microwave LO source to obtain the Brillouin spectrum of the system.

2.3 | Major parameters in BOTDR systems

Important indicators in the performance of the BOTDR system include the SNR, the spatial resolution, the frequency accuracy, the sensing range, and the measurement speed etc.

However, there is a trade-off relationship between these important parameters.

2.3.1 | Spatial resolution

Spatial resolution is an important indicator and refers to the shortest operation length at which the information in a segment of the fibre can be detected. If the incident optical wave is a pulsed signal with a pulse width of τ , the spatial resolution can be calculated as:

$$\Delta z = \frac{\tau c}{2n_{\text{eff}}} \quad (11)$$

which means the spatial resolution is directly related to the probe pulse width. However, in the conventional BOTDR systems, the spatial resolution cannot be improved indefinitely and is practically limited to 1 m, because a narrow pulse will cause a broader spectral distribution when the injected pulse width is shorter than the double phonon lifetime of about 10 ns, and the relationship between the FWHM of the Brillouin spectrum and the pulse width is given in Ref. [34]

$$\omega = \frac{2\sqrt{2}}{\pi T} \quad (12)$$

2.3.2 | Frequency error

The total noise in BOTDR systems is brought about by the inescapable digitiser noise from the transmitter and the receiver, the amplified spontaneous emission noise from the EDFA, and the thermal noise from the laser. The Brillouin spectrum frequency resolution is a parameter to evaluate the accuracy of the Brillouin spectrum. For a higher SNR, the frequency error $\delta\nu_B$ is exactly dropped, which can be approximated as follows [35]

$$\delta\nu_B = \frac{\omega}{\sqrt{2}(\text{SNR})^{1/4}} \quad (13)$$

This approximate solution suggests that the frequency error is proportional to the FWHM of the Brillouin spectrum.

2.3.3 | Sensing range

Since the loss occurs when the probe pulse propagates through the fibre, the detector cannot receive the power of the backscattered light when the transmission distance is extremely long. Such a limit on transmission distance is described as the sensing range. Increasing the inject pump power of the probe pulse can compensate for the fibre loss. However, a high enough power above the non-linear threshold of the probe pulse will boost the SBS thus leading to significant degradation of the pump power. A narrow probe pulse

will contribute to a high spatial resolution, but there is still a limitation on the sensing range, due to the low power of the narrow pulse.

2.3.4 | Measurement speed

In conventional BOTDR systems, frequency scanning configuration is generally the most essential component to capture the Brillouin frequency spectrum at each frequency shift point step by step. The method of averaging N signals increases the measurement time while improves the SNR of the system. The measurement time can be described as [36]:

$$T_{\text{total}} = N_{\text{avg}} \cdot N_{\text{freq}} \cdot \frac{2nL}{c} \quad (14)$$

where N_{avg} is the number of average signals, N_{freq} is the number of frequency scanning steps, L is the whole length of the test fibre, and the factor $\frac{2nL}{c}$ represents the travelling time of the probe pulse in test fibre.

3 | SINGLE PROBE PULSE MODULATION

The development and the use of EOMs, especially Mach-Zehnder modulators (MZMs), have led to great advances in the pulse modulation technology. Characteristics such as the duration and the shape of a single pulse can pose significant impacts on the performance of the system. This section reviews the recent design in the amplitude and the phase of a single pulse in the BOTDR system, as well as corresponding effects on the system performance.

3.1 | Duration and time interval modulation

As we discussed above, there is a trade-off between the spatial resolution and the frequency accuracy in the BOTDR system. The pulse width has an important effect on the spatial resolution. To avoid spectral broadening caused by the narrow pulse, the intensity modulation and the phase modulation methods are utilised in BOTDR systems to control the duration and time interval of the pulses. These modifications in pulses can improve the spatial resolution to the centimetre level.

3.1.1 | Double-pulse BOTDR

Double-pulse BOTDR (DP-BOTDR) was the first proposed technique to improve the spatial resolution of the BOTDR system to less than 1 m by modulating the during time and the intermittent time of the probe pulse in 2008 [37]. The probe pulse, modulated by an EOM and a pulse generator, was composed of two short pulses with the widths of 2 ns and the

interval time (between the two pulses) of 5 ns, as shown in Figure 4a. A baseband filter was placed behind the balanced photodetector at the receiver to capture the interference between the two optical pulses. The peak frequency of the Brillouin backscattered signal from the two narrow-width pulses, that is, the BFS, can be obtained using the spectral oscillation property generated via this interference. The results have shown that within a 50 m sensing range, DP-BOTDR can achieve a 20-cm spatial resolution with a BFS error of 1 MHz, corresponding to a strain error of $20 \mu\epsilon$ or a temperature error of 1°C [38].

3.1.2 | Synthetic BOTDR

A synthetic spectrum approach for BOTDR using quadrature-phase modulation technique was proposed in 2014, called synthetic BOTDR (S-BOTDR) [39]. The system used two pulses with two matched filters. The pulse widths of the two pulses were D_1 and D_2 respectively ($D_1 < D_2$), in which D_1 was utilised to attain the less spatial resolution and D_2 was longer than the lifetime of acoustic phonons in the optical fibre to reach a satisfying frequency resolution. The amplitude ratio of the two pulses was r and the phase difference between the two pulses was θ . Similarly, the low-pass filters with a phase difference of ϕ were used to receive the four Brillouin backscattered spectral signals generated by the two pulses. The spatial and the frequency resolutions of the spectrum were greatly improved via the addition or the reduction of these signals. Researchers deployed three groups of probe pulse pairs with different parameters D_1 , D_2 and r into the S-BOTDR systems. In the case of $D_1 = 1.6$ ns, $D_2 = 50$ ns, $r = 0.093$, the spatial resolution can reach 10 cm with a 39.2 MHz line-width of the composite Brillouin spectrum along a 40 m FUT.

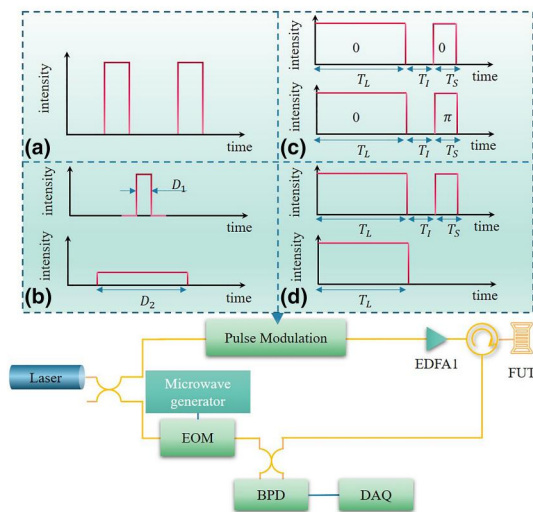


FIGURE 4 Single pulse modulation methods in BOTDR. (a) DP-BOTDR. (b) S-BOTDR. (c) PSP-BOTDR. (d) DCS-BOTDR. DAQ, data acquisition card.

3.1.3 | Two-step-subtraction BOTDR

In 2016, a method named two-step-subtraction was proposed to extract Brillouin spectral information with high spatial resolution using the tiny pulse width difference of a set of pulse pairs [40]. The process is shown in Figure 5. Fast Fourier transform (FFT) method of different time sequences were performed on each pulse in the pulse pair to obtain the four corresponding Brillouin spectra. The differential Brillouin spectrum with high spatial resolution was obtained by adding and subtracting these four spectra for two steps. However, the signal level of the differential spectrum with the pulse width difference $\Delta\tau$ of the two pulses was reduced to $(\Delta\tau/\tau)^2$ than the signal level of the single pulse with the pulse width τ . In order to ensure that the SNR and the frequency error of the system are within a suitable range, Li et al. conducted experiments with a 60/56 ns pulse pair, and obtained a spatial resolution of 0.4 m and a Brillouin frequency error of 4.1 MHz over a sensing range of 7.8 km.

A similar method utilising the extremely short pulse width difference $\Delta\tau$ between two pulses was proposed by Yu et al. in 2018. The method subtracted the information of the two pulses at each position of the fibre, and performed FFT on the subtracted information to obtain a Brillouin spectrum with sub-metre spatial resolution. The rise time and the fall time of the pulses were considered in the experiments. The experiment achieved a spatial resolution of 20 cm on a 3 km FUT, and proved that the longer rise time of the pulse can improve the SNR and the frequency error of the system [41].

3.1.4 | Phase-shift pulse BOTDR

Phase-shift pulse BOTDR (PSP-BOTDR) uses the quadrature-phase modulation technique to modulate a pair of detection pulses to detect the Brillouin backscattered lightwave information respectively. The two pulses in the probe pulse pair consisted of a long pulse and a short pulse and have the same duration and time intervals between each other, as illustrated in Figure 4c. The phase difference with a value of ϕ between the two short pulses enabled high spatial resolution information determined by the segment duration when the Brillouin signals detected by the two pulses were subtracted. The existence of the long pulses maintained the bandwidth of the Brillouin spectrum at a narrow level [42]. The PSP-BOTDR system, which utilised a long pulse of $T_L = 32$ ns

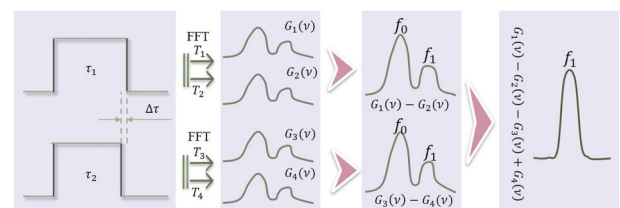


FIGURE 5 The scheme of two-step-subtraction technique in BOTDR system. BOTDR, Brillouin optical time-domain reflectometry.

and a short pulse of $T_S = 2$ ns with an interval of $T_I = 0.5$ ns, achieved a 20 cm spatial resolution along a 354.4 m FUT, with the frequency accuracy of 1.08 MHz [43].

3.1.5 | Differential cross spectrum BOTDR

To alleviate the Brillouin spectral error arising from the unbalanced light intensity between the 0-phase pulse and the ϕ -phase pulse caused by the pulse modulation process in the PSP-BOTDR system, a differential cross spectrum BOTDR (DCS-BOTDR) was proposed utilising the intensity modulation scheme to enhance the spatial resolution. Both pulses in the pulse pair contained a long pulse with a pulse width of T_L , and one of them had a short pulse with a pulse width of T_S subsequent to the long pulse with an interval time T_I , as shown in Figure 4d. At each point of the fibre, the information of the two pulses was collected by different window functions and subtracted. The subtracted information was processed by the FFT method to obtain the differential cross-correlation spectrum of the system. It is proved theoretically and experimentally that the differential cross-correlation spectrum obtained by this method could improve the spatial resolution of the system. Zan et al. obtained a spatial resolution of 0.2 m and a frequency error of 3.2 MHz on a 350 m fibre under test using a set of pulse pairs with parameter $T_L = 20$ ns, $T_I = 0.5$ ns, and $T_S = 2$ ns [44]. Further research on the performance of the DCS-BOTDR system has been carried out recently. Zan et al. compared the effect of different pulse duration on the performance of the DCS-BOTDR system and found that when $T_L = 14$ and 22 ns the system can achieve a better BFS resolution [45].

In 2022, the performance of the DCS-BOTDR system was further improved. Artificial neural network (ANN) has the characteristics of fast computation speed and can handle non-linear operations, and is thus suitable for fitting the BFS in the optical fibre. Almoosa et al. used Brillouin spectral data with a dimension of 1024×3000 as the input to train the network and improved the weight and the bias values according to the Levenberg-Marquardt optimisation. Then they deployed different combinations of probe pulses with $T_L = 2, 4, 14,$ and 60 ns into the DCS-BOTDR system respectively. The obtained BFS distributions were tested via the trained ANN model. Results demonstrated that the ANN model was effective in improving the BFS resolution and can obtain a 20 cm spatial resolution at the same time [46].

3.2 | Pulse shape modulation

In traditional BOTDR systems, rectangular pulses are usually modulated for the Brillouin spectrum detection. The Brillouin power spectrum is the convolution of the pulse and the spontaneous Brillouin scattering in the time domain, that is, the product between the pulse power spectrum and the standard Brillouin power spectrum in the frequency domain [47]. The Brillouin spectrum of a rectangular pulse produces side lobes

that reduce the peak power of the Brillouin power spectrum, resulting in a degradation in the SNR of the system. Commonly used pulses with different shapes are shown in Figure 6. In 2012, Hao et al. used an AOM to modulate rectangular pulses, triangular pulses and trapezoidal pulses with the same FWHM and the same peak power, and compared the Brillouin power spectrum according to the three pulses. The results show that the use of triangular and trapezoidal waves can significantly improve the SNR of the system [48, 49]. In 2016, Luo et al. deployed rectangular, Lorentzian, Gaussian and triangular pulses in a short-time Fourier transform BOTDR (STFT-BOTDR) system. The results show that rectangular pulses in STFT-BOTDR can improve the spatial resolution of the system, while Lorentzian pulses can improve the frequency resolution. Gaussian pulses had a more balanced resolution in the time and frequency domains [50]. In 2020, Hao et al. conducted theoretical and experimental analyses on the Brillouin spectra of pulses with three shapes (Lorentzian, Gaussian, and rectangular) under different laser spectral line-widths. It has proven that the use of Lorentzian pulses can increase the intensity of the Brillouin spectrum and reduce the frequency fluctuation of the BOTDR system [51].

In the current BOTDR system, the EOM is often used to modulate the continuous wave into a pulse wave. Extinction ratio (ER) is a parameter to monitor the quality of the probe pulse, and its stability will be affected by the temperature drift of the EOM. The ER of the pulse also has a remarkable influence on the SNR and the frequency error of the BOTDR detection system. In 2014, Zhang et al. reported a configuration of a high-ER probe pulse generator assisted by a synchronised optical switch. It was found that when the ER of the probe pulse was increased from 35 to 65 dB, the temperature uncertainty decreased from 5.2 to 0.8°C [52]. In 2018, Bai et al. used the gain switch modulation method to increase the pulse ER to 51.26 dB, which extended the sensing distance from 10.75 to 27.5 km with a spatial resolution of 1 m. Furthermore, at the position of 9.941 km in the FUT, the root-mean-square (RMS) error of BFS decreased from 2.49 to 0.78 MHz, and the fluctuation range decreased from 7.84 to 2.76 MHz [53]. In 2020, Liang et al. proposed a gain switch formation based on the semiconductor optical amplifier to improve the ER of the probe pulse. Compared to the traditional BOTDR system based on EOM modulation, this structure can improve the ER of probe pulse from 33.28 to 51.15 dB and improve the stability of the BFS measurement [54]. In 2021, Li et al. deduced a theoretical model of the

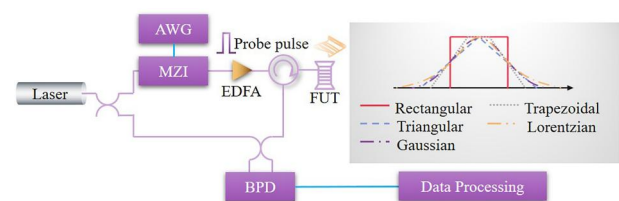


FIGURE 6 Different modulated pulses with the same pulse width. AWG, arbitrary waveform generators; MZI, Mach-Zehnder interferometer.

relationship between the ER of probe pulse and the SNR in BOTDR systems. Theoretical and experimental results suggested that SNR will increase with the ER. When the value of ER exceeded 50 dB, the pulse was close to the ideal pulse, and the SNR of the system was also close to its maximum [55].

4 | CODING IN BOTDR

As mentioned in Section 2.3, the SNR of the system can be improved by averaging N signals of the single pulses at the expense of the measurement speed. Pulse coding techniques are proven as an effective method to improve the SNR by injecting a pulse sequence with a code length of L . This leads to a higher power for the incident signals compared to a single pulse case, at the same time maintains the spatial resolution and reduces the measurement time. The quality of a pulse coding system can be expressed by the coding gain, which is defined as the ratio of the SNR obtained by the coded pulse to the SNR obtained by a single pulse under otherwise identical conditions. The coding gain depends on the coding length but is different for various coding schemes. The current schemes of coding sequences can be distinguished into two types: the complementary sequences for example, Golay sequences and linear combination sequences, for example, Simplex sequences or Hadamard sequences. Recently a random pulse coding scheme has been proposed, which has also been validated in improving the performance of the system. The encoding and decoding principles of different sequences are shown in Figure 7 and described in detail in this section.

4.1 | Complementary sequences

Golay complementary sequences are comprised of two different sequences A_k and B_k with the same bit length, and

Golay bits include 1 and -1 . A certain complementary relationship exists between the two sequences, which can be described as [56]:

$$c_j = \sum_{n=0}^{L-j-1} a_n a_{n+j} \quad (15)$$

$$d_j = \sum_{n=0}^{L-j-1} b_n b_{n+j} \quad (16)$$

$$c_j + d_j = 0 (j \neq 0); \quad (17)$$

$$c_0 + d_0 = 2L \quad (18)$$

where a_n and b_n are the values of the elements in the A_k and B_k sequences respectively. The two bipolar signals will be dismantled to four uni-polar sequences as U_k , \bar{U}_k , W_k and \bar{W}_k , loading on the inject lightwave as pulse sequences respectively. The decoding process is actually to solve the impulse response function h_k of the system. The four pulses are fed to the optical fibre independently. Data acquisition and processing unit accept four sets of signals and has a correlation operation before averaging them. The demodulation process is described as follows:

$$X_k = A_k * (U_k \otimes h_k - \bar{U}_k \otimes h_k) \quad (19)$$

$$Y_k = B_k * (W_k \otimes h_k - \bar{W}_k \otimes h_k) \quad (20)$$

$$Z_k = X_k + Y_k = 2L\delta_k \otimes h_k \quad (21)$$

where \otimes is the convolution calculation, and $*$ is the correlation calculation. Equation (21) illustrates that the final response of this algorithm is $2L$ times to the signal pulse system. The SNR

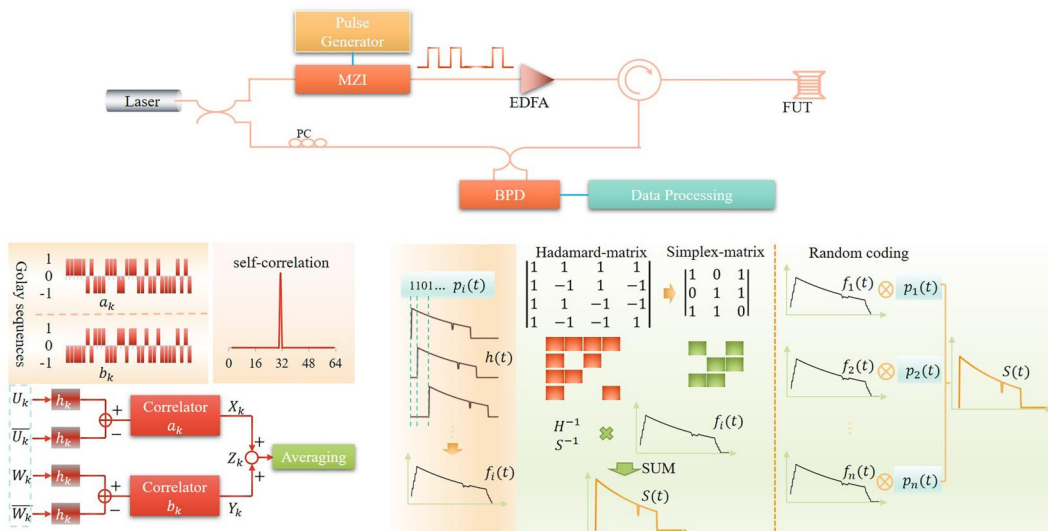


FIGURE 7 Different pulse coding techniques in BOTDR systems. BOTDR, Brillouin optical time-domain reflectometry

of the BOTDR based on Golay coding is $\sqrt{L}/2$ times higher than that in the traditional BOTDR system.

In 2012, Li et al. simulated the performance of BOTDR system based on Golay sequence coding. The Brillouin signal intensity of the BOTDR system using the 64-bit Golay complementary sequence is 128 times higher than that of the single-pulse BOTDR system, and the SNR and the spectral resolution of the system were significantly improved [57]. In 2017, Wang et al. combined Golay coding sequence with FFT technology to improve the system SNR and at the same time to increase the measurement speed. The trade-off between measurement accuracy, spatial resolution and measurement speed was well solved [58]. In 2020, Zan et al. deployed Golay code sequences into DCS-BOTDR systems. This method fused Golay code complementary sequences with two pulse sequences consisting of long and short pulses. The Brillouin spectrum along the fibre optic cable was extracted using FFT-based cross-spectral calculations to produce narrow Brillouin spectral widths contributed by long pulse durations. The spatial resolution of the system was improved to 40 cm determined by the difference between the long and the short pulses, and the BFS resolution was improved from 6.28 to 3.47 MHz along a 1280 m FUT [59]. In 2020, Li et al. studied the effect of using Golay coding sequence on the performance of BOTDR system under radiation environment. The Brillouin gain spectra of single-pulse, 16-, 32- and 64-bit Golay coded pulse sequences were obtained under different radiation dose. The results show that the use of 64-bit Golay code can effectively improve the sensing range and measurement accuracy of the BOTDR system in the radiation environment, but the increase of the code length will increase the complexity of the system [60].

4.2 | Linear combination sequences

4.2.1 | Hadamard sequences

Hadamard sequences is generated by the Hadamard matrix H of order n , which has the characters following properties: The element in H-matrix are merely 1 and -1 , and it satisfies the condition: $HH^{-1} = nI_n$, where I_n is the identity matrix with the order n . When a single pulse is injected into the optical fibre, the coded traces $s(t)$ measured by injected Hadamard sequence can be expressed as:

$$\begin{pmatrix} s_1(t) \\ s_2(t) \\ \vdots \\ s_n(t) \end{pmatrix} = H \begin{pmatrix} u_1(t) \\ u_2(t) \\ \vdots \\ u_n(t) \end{pmatrix} + \begin{pmatrix} n_1(t) \\ n_2(t) \\ \vdots \\ n_n(t) \end{pmatrix} \quad (22)$$

where $n_i(t)$ is the noise term among the transmission. The measured traces processed using the inverse Hadamard transform is expressed by

$$\begin{pmatrix} \hat{u}_1(t) \\ \hat{u}_2(t) \\ \vdots \\ \hat{u}_n(t) \end{pmatrix} = H^{-1} \begin{pmatrix} s_1(t) \\ s_2(t) \\ \vdots \\ s_n(t) \end{pmatrix} \quad (23)$$

where $\hat{u}_i(t)$ is the estimate of $u_i(t)$. Considering the pulse width τ , the estimated time-domain trace of the $u(t)$ can be obtained by averaging $u_i(t)$ after the time-shifting:

$$\hat{u}(t) = \frac{\hat{u}_1(t) + \hat{u}_2(t + \tau) + \dots + \hat{u}_n(t + (n-1)\tau)}{n} \quad (24)$$

which is utilised to reduce the effect of the noise on the signal. The coding gain that can be obtained using the Hadamard sequence is $(N+1)/(2\sqrt{N})$. In 2010, Lu et al. launched a 16-bit Hadamard sequence of probe pulses on the BOTDR system over a 37 km fibre and demonstrated the improvement effect of this method on the system SNR [61].

4.2.2 | Simplex sequences

Simplex coding sequence is a type of unipolar sequences derived by H matrix using the element 0 to replace the -1 in H matrix and deleting the first row and first column of H matrix. The demodulation principle of simplex coding method is similar to Hadamard coding to achieve the estimated time-domain trace. The coding gain of Simplex coding is $(N+1)/(2\sqrt{N})$, where N is the order of the Simplex matrix [62]. In 2008, Soto et al. used a MZM to deploy a 127-bit Simplex code in an OTDR-based Brillouin-based distributed temperature sensor using the Landau Placzek ratio. A coding gain of 7 dB was obtained experimentally, while the theoretical value was estimated as 7.54 dB. The temperature resolution was improved from 46.4 to 5.0 K at a 30 km FUT with a 42 m spatial resolution [63, 64]. In 2012, Fan et al. used simplex code to design a dedicated hardware system with field programmable gate array to reduce the time cost of the BOTDR system. The processing algorithm was optimised to improve the coding/decoding time on the basis of improving the SNR of the system [65]. In 2014, Hao et al. deployed a 31-bit simplex code in the BOTDR system using digital coherent detection technology without a frequency sweep device. Compared to the single-pulse system, the frequency error was optimised by 14.103 MHz, and the SNR was improved by 3.5 dB [66].

4.3 | Random coding

In 2020, a novel random coding method for the BOTDR system was proposed by Wang et al. [22]. The time domain characteristics of random coding show a distribution balance, which means that when the sequence has enough bits, the numbers of '1' and '0' are roughly equal. The self-correlation property of random coding sequence can be described as:

$$\eta(t) = \frac{\sum_{i=1}^M p_i(t) \otimes [p_i(t) - \bar{p}_i(t)]}{M} = \frac{L}{4} \cdot \delta(t) \quad (25)$$

The signal decoding process is realised by the cross-correlation between the backscattered light and the detection coding sequence. Therefore, the $S(t)$ can be obtained by the cross-correlation operation between the Brillouin backscattered signal and its corresponding detection random pulse sequence as:

$$\begin{aligned} S(t) &= \frac{\sum_{i=1}^M S_i(t)}{M} = \frac{\sum_{i=1}^M p_i(t) \otimes [f_i(t) - \bar{p}_i(t)]}{M} \\ &= h(t) * \frac{L}{4} \delta(t) \end{aligned} \quad (26)$$

It can be seen from the above formula that the response function of a single pulse can be calculated as

$$h(t) = \frac{4}{L} \cdot S(t) \quad (27)$$

Compared to the single-pulse BOTDR system, using the random coded pulse sequence for detection can improve the SNR of the system to $\sqrt{2L}/2$ times and can reduce the frequency resolution of the 4.93 km fibre from 5.34 to 0.38 MHz. Additionally, the random coding can improve the sensing range of a BOTDR system while maintaining the spatial resolution, at the same peak power as the single-pulse BOTDR system.

5 | FREQUENCY MODULATION IN BOTDR

5.1 | Broad-band laser using in BOTDR

Generally, BOTDR systems mostly adopt the local heterodyne structure in the detection. The use of narrow-linewidth lasers ensures the high precision in the BFS obtained from the coherent detection of the local reference light and the spontaneous Brillouin scattered light. In 2017, Li et al. proposed a BOTDR system employing the self-heterodyne detection of the Rayleigh and the Brillouin scattering, as shown in Figure 8. The impacts of laser sources with

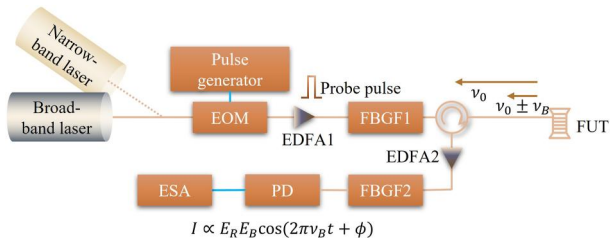


FIGURE 8 The setup of BOTDR using narrow-band laser and broad-band laser based on self-heterodyne detection. BOTDR, Brillouin optical time-domain reflectometry; ESA, electrical spectrum analyser; FBGF, fibre Bragg grating filter; PD, photodetector.

different frequency stabilities on the local-heterodyne and self-heterodyne detection systems were compared, and the feasibility of the broad-band laser source and the heterodyne detection method in the BOTDR system has been demonstrated. Results showed that the use of broad-band laser in the self-heterodyne detection system can effectively eliminate the adverse effects of the laser frequency instability on the system performance. Compared to the local heterodyne detection system, the maximum temperature errors measured by the narrow-band laser and the broad-band laser based on the self-heterodyne BOTDR system are reduced from 5.3 and 7.9°C to 2.4 and 1.2°C respectively [67, 68].

5.2 | Wavelength multiplexing technique

A conventional BOTDR system generally works with a narrow bandwidth laser source to clearly measure the Brillouin spectrum. In 2009, a BOTDR system was proposed by Soto et al. with a multi-longitudinal mode FP laser to emit the multi-wavelength rays, as shown in Figure 9. The wavelength spacing of the FP laser was larger than the bandwidth of the Brillouin scattering spectrum. The use of the multi-longitudinal mode FP laser led to the enhancement of the threshold value of the injected peak power to avoid the non-linear effects because the threshold for the SBS scheme limited only the peak laser power per mode. At the same time, the 127-bit Simplex pulse sequences was also deployed using a Mach-Zehnder interferometer. The configured FP laser had a 10 nm linewidth, 15 dBm input power, and 350 ns pulse width. Experimental results show that the system achieved a temperature resolution of 4.5 K and a strain resolution of 115 $\mu\epsilon$ for simultaneous measurement at 25 km distance [69].

In 2017, Lalam et al. used an MZM to modulate the single-wavelength ray output from a tunable laser, to produce rays with three pump wavelengths into the system. The two side-band rays, with a 5 GHz frequency shift to the carrier, had the same peak power as the carrier light. The obtained spectra of the three pump signals was combined as an enhanced Brillouin gain spectrum. The proposed structure, called wavelength diversity BOTDR, achieved an improvement in the SNR and the measurement accuracy by 3.92 dB and 3.6 times, respectively, compared to the traditional single-wavelength BOTDR scheme [70]. In 2018, Lalam used the Brillouin ring laser (BRL) at the LO path into a BOTDR system with the wavelength diversity

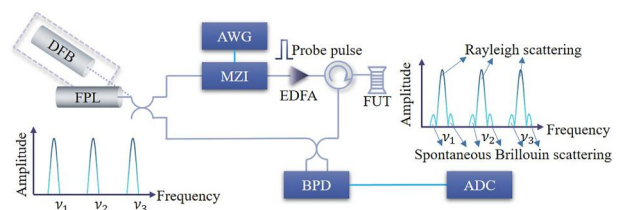


FIGURE 9 A wavelength-division multiplexing technique based on Fabry-Perot laser. ADC, analog-to-digital converter; DFB, distributed feedback laser; FPL, Fabry-Perot laser.

technique to eliminate the enormous BFS uncertainty of different pump wavelengths. The setup of the system is illustrated in Figure 10. A tunable distributed feedback (DFB) laser was utilised and the frequency shift in test fibre and BRL are $\nu_k - \nu_B$ and $\nu_k - \nu_{B-LO}$, where $k = 1, 2, 3$. At the receiver, three Brillouin gain spectra with the frequency as $\nu_B - \nu_{B-LO}$ were obtained via coherent detection and superimposed as proportional to the sensor amplitude response. Along a 50 km optical fibre, the system achieved an SNR improvement of 4.92 dB and stain or temperature accuracy of $0.05 \text{ MHz}/\mu\text{E}$ and $1.07 \text{ MHz}/^\circ\text{C}$ [71, 72].

In 2020, Wang et al. employed a multi-frequency probe pulse into the self-heterodyne detection BOTDR system to improve the performance of the system. A phase modulator is utilised to excite the multifrequency probe light with three frequencies and the frequency interval is set as 500 MHz. To eliminate the effect of coherent Rayleigh noise in the system, a frequency shift-averaging method is proposed by shifting the central frequency of the laser source and averaging the

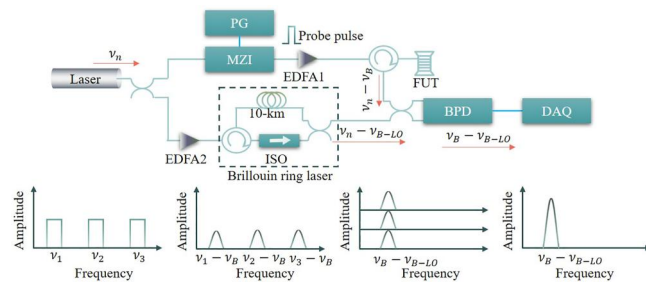


FIGURE 10 Wavelength diversity technology based on Brillouin laser ring. ISO, isolator; PG, pulse generator.

measurement signals to obtain the final self-heterodyne detection signals. The results show that the SNR of the Brillouin spectrum obtained by multi-frequency pulses with 22-time shift-averaging at the end of a 50 m fibre is increased by 7.92 dB and the amplitude fluctuation is reduced by 0.846 dB compared with the Brillouin spectrum measured by a single-frequency pulse without any averaging. And the highest accuracy of temperature measurement achieved 0.36°C using the three-frequency probe pulse and the shift-averaging [73].

5.3 | Pulse compression

Pulse compression (PC) is commonly used in radar ranging, communication, and other fields. The significant elements in PC technique are the chirp pulse using LFM and the matched filter with a response of the inverse conjugate on the time axis of the incident wave. As shown in Figure 11a, a narrow pulse which amplitude is as a sinc-shape function is generated by the convolution of the returned chirp pulse and the impulse response of the matched filter. The peak power position on the time axis of the compressed pulse refers to the position of the chirp pulse returning. For distributed optical fibre sensing systems based on the scattering in optical fibre, the distance detection method is similar to the radar system via the return time of the probe pulse. It has proved that the PC technique is of efficiency to improve the spatial resolution in DOFS systems [25, 75–77]. In 2021, Xu et al. proposed a BOTDR based on a bipolar-chirped pulse pair and named it as the BPP-BOTDR. The feasibility of the LFM technology in BOTDR systems was tested both theoretically and practically [74]. When the chirp probe pulse is injected into the FUT, the scattered light can be expressed as

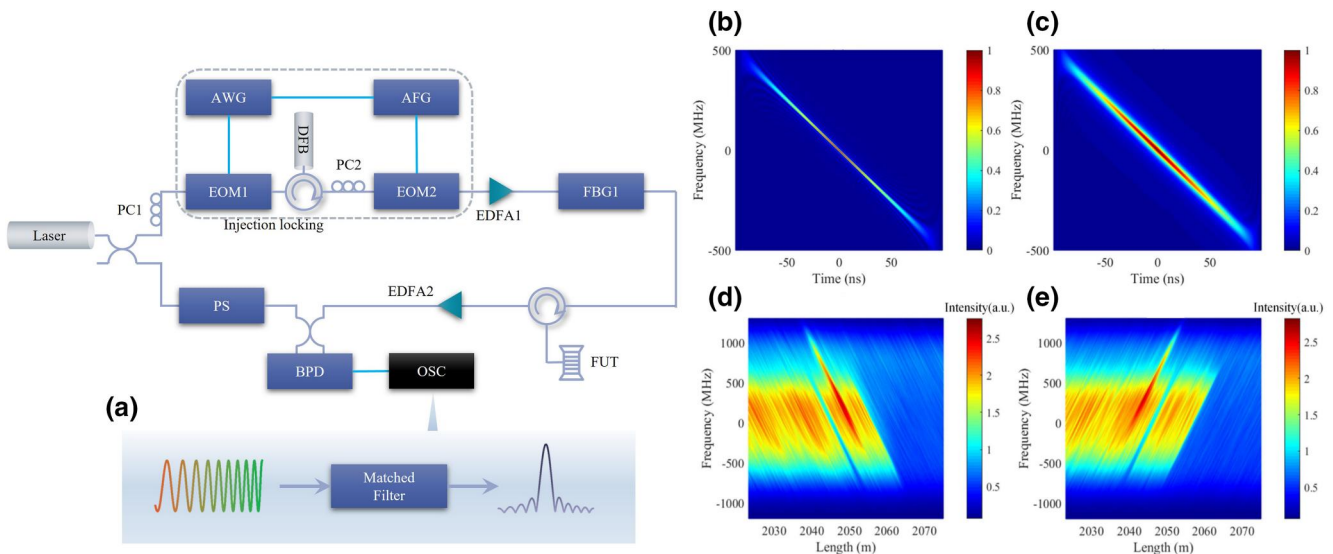


FIGURE 11 Setup and experimental results of BPP-BOTDR [74]. (a) Principle of pulse compression via a matched filter. (b) Time–frequency spectral maps of a single point of the PC obtained for Rayleigh scattering. (c) Time–frequency spectral maps of a single point of the PC obtained for Brillouin scattering. (d) Brillouin time–frequency spectrum along a 2056 m fibre with a 500 MHz BFS obtained by a positive-chirped pulse. (e) Brillouin time–frequency spectrum along a 2056 m fibre with a 500 MHz BFS obtained by a negative-chirped pulse. AFG, arbitrary function generator; BFS, Brillouin frequency shift; FBG, fibre Bragg grating; OSC, oscilloscope; PC, pulse compression; PS, polarisation scrambler.

$$E_B(t) = E_0 \text{rect}\left(\frac{t}{T}\right) \int_{-\infty}^{+\infty} g(\nu_B, \Delta\nu_B, \nu) e^{j2\pi(\nu+\nu_B)t + j\pi k t^2} d\nu \quad (28)$$

where T is the pulse width, k is the frequency modulation rate as $k = B/T$, and B is the modulation bandwidth. The reference signal can be described as $E_R(t) = E_R e^{j2\pi\nu_r t}$. Accordingly, the signal in the balanced photodetector is described as follows:

$$s(t) = E_0 E_R \text{rect}\left(\frac{t}{T}\right) \int_{-\infty}^{+\infty} g(\nu_B, \Delta\nu_B, \nu) e^{j2\pi(\nu+\nu_r)t + j\pi k t^2} d\nu \quad (29)$$

where $\nu' = \nu_B - \nu_r$, with a bandwidth of several hundreds of MHz, represents the frequency difference between the signal and the reference ray via the balanced detector in the traditional BOTDR system. Considering the matched filter with the response of

$$h(t) = s(-t)^* \quad (30)$$

$$x(t) = E_0 \text{rect}\left(\frac{t}{T}\right) \exp(j\pi k t^2) \quad (31)$$

The output signal from the matched filter can be calculated as:

$$\begin{aligned} |s_{out}| &= |s(t) \otimes h(t)| \propto \left| \text{rect}\left(\frac{t+T}{2T}\right) \int_{-\infty}^{+\infty} g(\nu_B, \Delta\nu_B, \nu) \right. \\ &\quad \times \left. \frac{\sin \pi k [t + (\nu + \nu')/k] (T - |t|)}{\pi k [t + (\nu + \nu')/k]} d\nu \right| \end{aligned} \quad (32)$$

Here, the $|s_{out}|$ describes the waveform of the compressed pulse as a sinc-like function in the regime of Brillouin scattering. The t in Equation (32) is a response to the scattering point in the optical fibre. Furthermore, the peak of the compressed pulse will be shifted along the time axis caused by the BFS and the bandwidth and the time duration of the chirp pulse which is reflected as the parameter $-\frac{(\nu+\nu')}{k}$.

The time-frequency spectrums of the compressed pulse for Rayleigh scattering and Brillouin scattering at a single point of the fibre are shown in Figure 11b,c. It shows that PC signals are skewed in the time-frequency plane expected as Equation (32). For the entire length of the fibre, the time-frequency spectrum of the BOTDR system refers to the order of the single-point information on the time axis. When a strain is loaded on the fibre with a BFS value of 300 MHz, the spectral map of the PC appears as a shift of the point on the frequency axis. To correct this degradation, a bipolar-chirped pulse pair and a cross-correlation-based demodulation method were utilised to achieve the precise positioning of the strain and a higher spatial resolution. The time-frequency spectrums obtained from the positive and negative chirped pulses are shown in Figure 11d,e respectively. Furthermore, the whole

Brillouin spectrum of the sensing fibre is acquired at one time to realise a real-time detection. However, the Brillouin spectrum of the FUT at a different position under various strains may overlap with each other, which increases the difficulty in the demodulation of various strain distributions. This means that the BPP-BOTDR still needs to be improved in practical engineering applications.

6 | CONCLUSION AND VISION

In this review, the recent progress of the probe pulse design in BOTDR systems has been discussed comprehensively. Due to the mutual constraints between various parameters, for example, spatial resolution, SNR, frequency measurement accuracy, sensing range, and measurement speed, in the BOTDR system, researchers changed the amplitude, the phase, the frequency and the sequence of the pulse to improve the performance of the BOTDR systems. For traditional single-pulse BOTDR systems, the spatial resolution is limited to be ~ 1 m, attributed to the limitation of the Brillouin spectral accuracy. To enhance the spatial resolution, DP-BOTDR, synthetic BOTDR, PSP-BOTDR, DCS-BOTDR, and two-step-subtraction BOTDR systems have been proposed by modulating the amplitude, the duration time and the phase of single- or dual-pulses respectively. LFM technique is used to launch a chirp pulse into the FUT. Combined with a matched filter it can improve the spatial resolution and realise a real-time distributed detection. Nevertheless, the BFS of strains at different points along the fibre will interfere each other, and thus the demodulation method of the BPP-BOTDR still needs to be investigated and improved.

The SNR is a system parameter closely related to the measurement accuracy and the sensing range, and can be improved by multiplying and averaging the output signals at the expense of the measurement speed of the system. It has been demonstrated that the shape and the ER of the probe pulse pose the effect on the SNR of the system. Pulse coding is currently the most popular technology to improve the SNR. This method feeds multiple groups of optical pulses with coded sequences into the system, and decodes the output results, which can obtain higher system performance gain, depending on the number of pulse sequences. In addition, the frequency division multiplexing has also been implemented into the BOTDR system to enhance the SNR.

For the future development of the probe pulse design, higher-order pulse coding formats are expected to be used in BOTDR systems. High-order pulse coding formats have been widely used in high-speed optical fibre communication systems to increase the transmission capacity. Some researchers have deployed the differential (DPSK) and quadrature phase shift keying modulation formats into the BOTDA systems, to improve the spatial resolution of the system [78]. The deployment of high-order modulation formats in distributed optical fibre sensing systems can also further promote the integration of optical fibre communication networks and

optical fibre sensing networks, which would bring great economic benefits [79, 80]. In recent years, new coding sequences are also under investigation to further enhance the SNR of the systems. More efficient pulse coding techniques will be implemented and applied. Chirped pulses generated by linear pulse modulators can also play an important role in improving the performance of BOTDR systems. The issue of the frequency crosstalk is expected to be resolved in the future. In addition, the combination of various pulse modulation techniques can also further improve the performance of the BOTDR systems.

AUTHOR CONTRIBUTIONS

Mupeng Li: Investigation (lead); Visualisation (lead); Writing – Original Draft Preparation (lead). **Tianhua Xu:** Conceptualisation (lead); Supervision (lead); Investigation (equal); Writing – Review & Editing (equal). **Shuang Wang:** Writing – Review & Editing (equal). **Wenxiu Hu:** Writing – Review & Editing (equal). **Junfeng Jiang:** Supervision (equal); Writing – Review & Editing (equal). **Tiegen Liu:** Supervision (equal); Writing – Review & Editing (equal).

ACKNOWLEDGEMENT

This research is supported by the National Natural Science Foundation of China (Grant No. 61735011) and H2020 Marie Skłodowska-Curie Actions (Grant No. 101008280).

CONFLICT OF INTEREST

No conflict of interest exists in the submission of this manuscript, and the manuscript is approved by all authors for publication.

DATA AVAILABILITY STATEMENT

Data sharing not applicable to this article as no data sets were generated or analysed during the current study.

ORCID

Tianhua Xu  <https://orcid.org/0000-0003-2659-7872>

Wenxiu Hu  <https://orcid.org/0000-0001-6215-6527>

REFERENCES

- Ou, J., Li, H.: Structural health monitoring research in china: trends and applications. In: *Structural Health Monitoring of Civil Infrastructure Systems*, pp. 463–516. Elsevier (2009)
- Monfared, Y.E.: Overview of recent advances in the design of plasmonic fiber-optic biosensors. *Biosensors*. 10(7), 77 (2020). <https://doi.org/10.3390/bios10070077>
- Pasche, S., et al.: Smart textiles with biosensing capabilities. *Adv. Sci. Technol.* 80, 129–135 (2013)
- Loyez, M., et al.: Cytokeratins biosensing using tilted fiber gratings. *Biosensors*. 8(3), 74 (2018). <https://doi.org/10.3390/bios8030074>
- Vidakovic, M., et al.: Fibre Bragg grating-based cascaded acoustic sensors for potential marine structural condition monitoring. *J. Lightwave Technol.* 34(19), 4473–4478 (2016). <https://doi.org/10.1109/jlt.2016.2587161>
- Vandenplas, S., et al.: Acoustic emission monitoring using a polarimetric single mode optical fiber sensor. In *17th International Conference on Optical Fibre Sensors*, vol. 5855, pp. 1064–1067. SPIE (2005)
- Borinski, J.W., et al.: Fiber-optic acoustic-emission sensors and detection. *Proc. SPIE*. 174(1), 92–96 (2000)
- Farahani, A.M., Gogolla, T.: Spontaneous Raman scattering in optical fibers with modulated probe light for distributed temperature Raman remote sensing. *J. Lightwave Technol.* 17(8), 1379–1391 (1999). <https://doi.org/10.1109/50.779159>
- Safaii-Jazi, A., Najafi, S.I.: Optical fibers and applications. *Opt Laser Technol.* 33(5), 277–278 (2001). [https://doi.org/10.1016/s0030-3992\(01\)00017-2](https://doi.org/10.1016/s0030-3992(01)00017-2)
- Murphy, K.A., et al.: Quadrature phase-shifted, extrinsic fabry-perot optical fiber sensors. *Opt. Lett.* 16(4), 273 (1991). <https://doi.org/10.1364/ol.16.000273>
- Homola, J., Yee, S.S., Gauglitz, G.N.: Surface plasmon resonance sensors: review. *Sensor. Actuator. B Chem.* 54(1–2), 3–15 (1999). [https://doi.org/10.1016/s0925-4005\(98\)00321-9](https://doi.org/10.1016/s0925-4005(98)00321-9)
- Kersey, A.D., Berkoff, T.A., Morey, W.W.: Fiber-optic bragg grating strain sensor with drift-compensated high-resolution interferometric wavelength-shift detection. *Opt. Lett.* 18(1), 72–74 (1993). <https://doi.org/10.1364/ol.18.000072>
- Hocker, G.B.: Fiber-optic sensing of pressure and temperature. *Appl. Opt.* 18(9), 1445–1448 (1979). <https://doi.org/10.1364/ao.18.001445>
- Lee, B.: Review of the present status of optical fiber sensors. *Opt. Fiber Technol.* 9(2), 57–79 (2003). [https://doi.org/10.1016/s1068-5200\(02\)00527-8](https://doi.org/10.1016/s1068-5200(02)00527-8)
- Lu, P., et al.: Distributed optical fiber sensing: review and perspective. *Appl. Phys. Rev.* 6(4), 041302 (2019). <https://doi.org/10.1063/1.5113955>
- Barnoski, M.K., et al.: Optical time domain reflectometer. *Appl. Opt.* 16(9), 2375–2379 (1977). <https://doi.org/10.1364/ao.16.002375>
- Rogers, J.A.: Polarization-optical time domain reflectometry: a technique for the measurement of field distributions. *Appl. Opt.* 20(6), 1060–1074 (1981). <https://doi.org/10.1364/ao.20.001060>
- Hartog, A.H., Leach, A.P., Gold, M.P.: Distributed temperature sensing in solid-core fibres. *Electron. Lett.* 23(21), 1061–1062 (1985). <https://doi.org/10.1049/el:19850752>
- Garus, D., et al.: Distributed sensing technique based on Brillouin optical-fiber frequency-domain analysis. *Opt. Lett.* 21(17), 1402–1404 (1996). <https://doi.org/10.1364/ol.21.001402>
- Kazuo, H., Hasegawa, T.: Measurement of Brillouin gain spectrum distribution along an optical fiber using a correlation-based technique - proposal, experiment and simulation. *IEICE Trans. Electron.* E83, 01 (2002)
- Horiguchi, T., Tateda, M.: Optical-fiber-attenuation investigation using stimulated Brillouin scattering between a pulse and a continuous wave. *Opt. Lett.* 14(8), 408–410 (1989). <https://doi.org/10.1364/ol.14.000408>
- Wang, Q., et al.: Random coding method for snr enhancement of BOTDR. *Opt Express.* 30(7), 11604 (2022). <https://doi.org/10.1364/oe.456620>
- Shimizu, K., et al.: Coherent self-heterodyne detection of spontaneously Brillouin-scattered light waves in a single-mode fiber. *Opt Lett.* 18(3), 185 (1993). <https://doi.org/10.1364/ol.18.000185>
- Ma, Z., et al.: Double-sideband heterogeneous pulse modulation method for distributed acoustic sensing. In: *2017 International Conference on Optical Instruments and Technology: Advanced Optical Sensors and Applications*, vol. 10618, pp. 33–39. SPIE (2018)
- Ma, Z., et al.: Phase drift noise suppression for coherent-otdr sensing based on heterogeneous dual-sideband lfm pulse. *APEX* 13(8), 082002 (2020). <https://doi.org/10.35848/1882-0786/aba152>
- Thévenaz, Lu.: *Advanced Fiber Optics*. Epfl Press (2011). <https://doi.org/10.1201/b16404:345-388>
- Naruse, H., Tateda, M.: Trade-off between the spatial and the frequency resolutions in measuring the power spectrum of the Brillouin back-scattered light in an optical fiber. *Appl. Opt.* 38(31), 6516 (1999). <https://doi.org/10.1364/ao.38.006516>
- Kurashima, T., et al.: Application of fiber optic distributed sensor for strain measurement in civil engineering. *Smart Mater. Struct. Integrated Syst.* 3241, 247–258 (1997)
- Parker, T.R., et al.: Temperature and strain dependence of the power level and frequency of spontaneous Brillouin scattering in optical fibers. *Opt Lett.* 22(11), 787 (1997). <https://doi.org/10.1364/ol.22.000787>

30. Barnoski, M.K., Jensen, S.M.: Fiber waveguides: a novel technique for investigating attenuation characteristics. *Appl. Opt.* 15(9), 2112–2115 (1976). <https://doi.org/10.1364/ao.15.002112>
31. Aoyama, K., Nakagawa, K., Itoh, T.: Optical time domain reflectometry in a single-mode fiber. *IEEE J. Quant. Electron.* 17(6), 862–868 (1981). <https://doi.org/10.1109/jqe.1981.1071237>
32. Akiyoshi, S., et al.: Development of integrated damage detection system for international America's cup class yacht structures using a fiber optic distributed sensor. In: *Smart Structures and Materials 2000: Sensory Phenomena and Measurement Instrumentation for Smart Structures and Materials*, vol. 3986, pp. 324–334. SPIE (2000)
33. Shimizu, K., et al.: Coherent self-heterodyne Brillouin OTDR for measurement of Brillouin frequency shift distribution in optical fibers. *J. Lightwave Technol.* 12(5), 730–736 (1994). <https://doi.org/10.1109/50.293961>
34. Alem, M., et al.: Analytical expression and experimental validation of the Brillouin gain spectral broadening at any sensing spatial resolution. In: *International Conference on Optical Fiber Sensors* (2017)
35. Soto, M.A., Thévenaz, L.: Modeling and evaluating the performance of Brillouin distributed optical fiber sensors. *Opt Express.* 21(25), 31347–31366 (2013). <https://doi.org/10.1364/oe.21.031347>
36. Bao, X., Zhou, Z., Wang, Y.: Distributed time-domain sensors based on Brillouin scattering and FWM enhanced SBS for temperature, strain and acoustic wave detection. *Photonix*. 2(1), 1–29 (2021). <https://doi.org/10.1186/s43074-021-00038-w>
37. Koyamada, Y., et al.: Novel type Brillouin optical time-domain reflectometry for measuring distributed strain and temperature with sub-meter spatial resolution in km-long fiber. In: *SICE Annual Conference 2007* (2008)
38. Sakairi, Y., et al.: Prototype double-pulse BOTDR for measuring distributed strain with 20-cm spatial resolution. In: *2008 SICE Annual Conference*, pp. 1106–1109. IEEE (2008)
39. Nishiguchi, K., et al.: Synthetic spectrum approach for Brillouin optical time-domain reflectometry. *Sensors.* 14(3), 4731–4754 (2014). <https://doi.org/10.3390/s140304731>
40. Li, Q., et al.: High spatial resolution BOTDR based on differential Brillouin spectrum technique. *IEEE Photon. Technol. Lett.* 28(14), 1493–1496 (2016). <https://doi.org/10.1109/lpt.2016.2555078>
41. Yu, Z., et al.: Distributed optical fiber sensing with Brillouin optical time domain reflectometry based on differential pulse pair. *Opt Laser. Technol.* 105, 89–93 (2018). <https://doi.org/10.1016/j.optlastec.2018.02.037>
42. Horiguchi, T., Masui, Y., Zan, M.S.D.: Analysis of phase-shift pulse Brillouin optical time-domain reflectometry. *Sensors.* 19(7), 1497 (2019). <https://doi.org/10.3390/s19071497>
43. Shibata, R., et al.: Improving performance of phase shift pulse BOTDR. *IEICE Electron. Express.* 14(11), 20170267 (2017). <https://doi.org/10.1587/ele.14.20170267>
44. Zan, M.S.D., Masui, Y., Horiguchi, T.: Differential cross spectrum technique for improving the spatial resolution of BOTDR sensor. In: *2018 IEEE 7th International Conference on Photonics (ICP)*, pp. 1–3. IEEE (2018)
45. Zan, M.S.D., et al.: The effect of pulse duration on the Brillouin frequency shift accuracy in the differential cross-spectrum BOTDR (DCS-BOTDR) fiber sensor. *Opt. Fiber Technol.* 72, 102977 (2022). <https://doi.org/10.1016/j.yofte.2022.102977>
46. Almoosa, A.S.K., et al.: Improving the Brillouin frequency shift measurement resolution in the Brillouin optical time domain reflectometry (BOTDR) fiber sensor by artificial neural network (ANN). *Opt. Fiber Technol.* 70, 102860 (2022). <https://doi.org/10.1016/j.yofte.2022.102860>
47. Hao, Y., et al.: Effects of modulated pulse format on spontaneous Brillouin scattering spectrum and BOTDR sensing system. *Opt Laser. Technol.* 46, 37–41 (2013). <https://doi.org/10.1016/j.optlastec.2012.04.025>
48. Hao, Y., et al.: Improvement of pulse shape on Brillouin optical time domain reflectometry. In: *OFS2012 22nd International Conference on Optical Fiber Sensors*, vol. 8421. 84219E. International Society for Optics and Photonics (2012)
49. Hao, Y., et al.: Theoretical research of influence of pump pulse rise/fall time on Brillouin optical time domain reflectometry. In: *Asia Communications and Photonics Conference*. M4A–193. Optical Society of America. (2019)
50. Luo, L., et al.: Time and frequency localized pulse shape for resolution enhancement in STFT-BOTDR. *J. Sens.* 2016, 1–10 (2016). <https://doi.org/10.1155/2016/3204130>
51. Hao, Y., et al.: Influence of pump pulse spectrum on the signal-noise-ratio of Brillouin scattering in Brillouin optical time domain reflectometry. *Opt. Fiber Technol.* 55, 102143 (2020). <https://doi.org/10.1016/j.yofte.2020.102143>
52. Zhang, Y., et al.: Performance enhancement for long distance BOTDR sensing system based on high extinction ratio probe pulse generator. In: *Optoelectronic Devices and Integration V*, vol. 9270, pp. 90–100. SPIE (2014)
53. Bai, Q., et al.: Enhancing the SNR of BOTDR by gain-switched modulation. *IEEE Photon. Technol. Lett.* 31(4), 283–286 (2018). <https://doi.org/10.1109/lpt.2018.2889812>
54. Liang, C., et al.: Stability enhancement of BOTDR strain sensing system by using soa-based-gain-switched modulation. In: *2020 IEEE 5th Optoelectronics Global Conference (OGC)*, pp. 143–146. IEEE (2020)
55. Li, J., et al.: Influence of probe pulse characteristics on snr of Brillouin optical time domain reflectometer. In: *Optics Frontiers Online 2020: Distributed Optical Fiber Sensing Technology and Applications*, vol. 11607. International Society for Optics and Photonics, 116070L (2021)
56. Cheng, X.W., Li, Y.Q.: Performance analysis of Brillouin optical time domain reflectometer using Golay complementary sequence. *Proc. SPIE* 6624 (2007)
57. Li, Y., Wang, J., Yang, Z.: A Method for Improving BOTDR System Performance. *IEEE* (2012)
58. Wang, F., et al.: Enhancing the performance of BOTDR based on the combination of FFT technique and complementary coding. *Opt Express* 25(4), 3504–3513 (2017). <https://doi.org/10.1364/oe.25.003504>
59. Zan, M., et al.: Pulse coding technique in differential cross-spectrum BOTDR for improving the Brillouin frequency accuracy and spatial resolution. In: *2020 IEEE 8th International Conference on Photonics (ICP)* (2020)
60. Li, M., et al.: Investigation on the improvement of Brillouin optical time-domain reflectometer with Golay pulse codes in radiation environment. *Opt. Eng.* 59(4), 046102 (2020). <https://doi.org/10.1117/1.oe.59.4.046102>
61. Lu, Y., et al.: Brillouin optical time-domain reflectometry based on Hadamard sequence probe pulse. In: *9th International Conference on Optical Communications and Networks (ICOON 2010)*. (2010)
62. Bolognini, G., et al.: Analysis of distributed temperature sensing based on Raman scattering using OTDR coding and discrete Raman amplification. *Meas. Sci. Technol.* 18(10), 3211–3218 (2007). <https://doi.org/10.1088/0957-0233/18/10/s24>
63. Soto, M.A., Bolognini, G., Di Pasquale, F.: 30-km spontaneous-Brillouin distributed temperature sensor employing simplex-coding and low optical input power. In: *SENSORS, 2008 IEEE*, pp. 282–285. IEEE (2008)
64. Soto, M.A., et al.: Brillouin-based distributed temperature sensor employing pulse coding. *IEEE Sensor. J.* 8(3), 225–226 (2008). <https://doi.org/10.1109/jsen.2007.913143>
65. Fan, Z., et al.: Design of fast pulse coding/decoding system for BOTDR. In: *2012 Photonics Global Conference (PGC)*, pp. 1–6. IEEE (2012)
66. Hao, Y.Q., et al.: Digital coherent detection research on Brillouin optical time domain reflectometry with simplex pulse codes. *Chin. Phys. B* 23(11), 253–256 (2014). <https://doi.org/10.1088/1674-1056/23/11/110703>
67. Li, Y., et al.: Detrimental effect elimination of laser frequency instability in Brillouin optical time domain reflectometer by using self-heterodyne detection. *Sensors.* 17(3), 634 (2017). <https://doi.org/10.3390/s17030634>
68. Li, X.J., et al.: Performance improvement of a self-heterodyne detection BOTDR system employing broad-band laser. *Optoelectron. Lett.* 14(5), 325–330 (2018). <https://doi.org/10.1007/s11801-018-8052-7>
69. Soto, M.A., Bolognini, G., Di Pasquale, F.: Distributed optical fibre sensors based on spontaneous Brillouin scattering employing multimode

- Fabry-Perot lasers. *Electron. Lett.* 45(21), 1071–1072 (2009). <https://doi.org/10.1049/el.2009.2381>
70. Lalam, N., et al.: Performance improvement of BOTDR system using wavelength diversity technique. In: 2017 25th Optical Fiber Sensors Conference (OFS), pp. 1–4. IEEE (2017)
 71. Lalam, N., et al.: Performance improvement of Brillouin ring laser based BOTDR system employing a wavelength diversity technique. *J. Lightwave Technol.* 36(4), 1084–1090 (2018). <https://doi.org/10.1109/jlt.2017.2766765>
 72. Lalam, N., et al.: Performance analysis of Brillouin optical time domain reflectometry (BOTDR) employing wavelength diversity and passive depolarizer techniques. *Meas. Sci. Technol.* 29(2), 025101 (2018). <https://doi.org/10.1088/1361-6501/aa9c6e>
 73. Wang, J., Li, Y., Zhang, L.: Performance enhancement for a self-heterodyne detection Brillouin optical time-domain reflectometer. *Opt. Eng.* 59(3), 034103 (2020)
 74. Xu, P., et al.: Fast acquirable Brillouin optical time-domain reflectometry based on bipolar-chirped pulse pair. *J. Lightwave Technol.* 39(12), 3941–3949 (2021). <https://doi.org/10.1109/jlt.2020.3042237>
 75. Loayssa, A., Sagues, M., Eyal, A.: Phase noise effects on phase-sensitive OTDR sensors using optical pulse compression. *J. Lightwave Technol.* 40(8), 2561–2569 (2021). <https://doi.org/10.1109/jlt.2021.3138249>
 76. Pastor-Graells, J., et al.: Snr enhancement in high-resolution phase-sensitive OTDR systems using chirped pulse amplification concepts. *Opt. Lett.* 42(9), 1728–1731 (2017). <https://doi.org/10.1364/ol.42.001728>
 77. Zou, W., et al.: Optical pulse compression reflectometry: proposal and proof-of-concept experiment. *Opt. Express.* 23(1), 512–522 (2015). <https://doi.org/10.1364/oe.23.000512>
 78. Stiller, B., et al.: Fiber optic Brillouin distributed sensing using phase-shift keying modulation techniques. In: *Optical Sensing and Detection II*, vol. 8439, pp. 61–69. SPIE (2012)
 79. Munster, P., et al.: Simultaneous transmission of the high-power phase sensitive OTDR, 100gbps dual polarisation QPSK, accurate time/frequency, and their mutual interferences. In: *Fiber Optic Sensors and Applications XIV*, vol. 10208, pp. 62–68. SPIE (2017)
 80. Ng, W.P., et al.: Integrating radio-over-fiber communication system and BOTDR sensor system. *Sensors.* 20(8), 2232 (2020). <https://doi.org/10.3390/s20082232>

How to cite this article: Li, M., et al.: Probe pulse design in Brillouin optical time domain reflectometry. *IET Optoelectron.* 1–15 (2022). <https://doi.org/10.1049/ote2.12081>